Heat and Mass Transfer (2018) 54:1301–1311
https://doi.org/10.1007/s00231-017-2230-1

ORIGINAL

Heat transfer and pressure drop studies of TiO_2/DI water nanofluids in helically corrugated tubes using spiraled rod inserts

S. Anbu[1] · S. Venkatachalapathy[1] · S. Suresh[1]

Received: 1 February 2017 / Accepted: 13 November 2017 / Published online: 24 November 2017

Abstract

An experimental study on the convective heat transfer and friction factor characteristics of TiO_2/DI water nanofluids in uniformly heated plain and helically corrugated tubes (HCT) with and without spiraled rod inserts (SRI) under laminar flow regime is presented in this paper. TiO_2 nanoparticles with an average size of 32 nm are dispersed in deionized (DI) water to form stable suspensions containing 0.1, 0.15, 0.2, and 0.25% volume concentrations of nanoparticles. It is found that the inclusion of nanoparticles to DI water ameliorated Nusselt number which increased with nanoparticles concentration upto 0.2%. Two spiraled rod inserts made of copper with different pitches (p_i = 50 mm and 30 mm) are inserted in both plain and corrugated tubes and it is found that the addition of these inserts increased the Nusselt number substantially. For Helically corrugated tube with lower pitch and maximum height of corrugation (p_c = 8 mm, h_c = 1 mm) with 0.2% volume concentration of nanoparticles, a maximum enhancement of 15% in Nusselt number is found without insert and with insert having lower pitch (p_i = 30 mm) the enhancement is 34% when compared to DI water in plain tube. The results on friction factor show a maximum penalty of about 53.56% for the above HCT.

Keywords TiO_2/DI waternanofluids · Laminar flow · Nusselt number · Corrugated tubes · Thermal performance factor

Nomenclature

A	cross-sectional area (m^2)
C_p	specific heat (J/kgK)
d	test section diameter (m)
f	friction factor
h	heat transfer coefficient (W/m^2K)
h_c	corrugation height (m)
I	current (A)
L	length of the test section (m)
m	mass flow rate (kg/s)
Nu	Nusselt number (hd/k)
Δp	pressure drop (N/m^2)
P	perimeter (m)
Pr	Prandtl number ($\mu C_p/k$)
p_c	corrugation pitch (m)
p_i	pitch of insert (m)
Q	heat input (W)
q″	heat flux (W/m^2)
R	thermal resistance ($°Cm^2/W$)
Re	Reynolds number (ρvd/μ)
T	temperature (K)
V	voltage (V)
v	fluid velocity (m/s)
X	Axial distance from the entrance (m)

Greek symbols

ρ	Density (kg/m^3)
μ	Dynamic viscosity (kg/m^2s)
∅	Volume concentration (%)

Subscripts

c	Corrugation
f	Fluid
i	Insert
in	Inlet
nf	Nanofluid
out	Outlet.
pt.	Plain tube
s	Solid phase
t	Total
w	Wall
x	Axial distance from the entrance (m)

Abbreviations

DI	Deionized
HCT	Helically Corrugated Tube
SRI	Spiraled Rod Insert

✉ S. Venkatachalapathy
svc@nitt.edu

[1] Department of Mechanical Engineering, National Institute of Technology, Tiruchirappalli 620015, India

1 Introduction

Nanofluids are generally obtained by dispersing nanometer sized particles in the base fluid. It has been researched and used for heat transfer augmentation for over two decade now. Nanofluids have proven to be of having immense potential in revolutionizing many industrial applications such as transportation, chemical industries, heating and cooling, power generation and electronic cooling. Heat transfer augmentation using nanoparticles was first done by Choi [1] in the year 1995 when the known microparticles did not prove to be effective in enhancing heat transfer rate. Since then a multitude of research has followed keeping Choi's work as the base. Al_2O_3, CuO, TiO_2 and SiO_2 are some of the nanoparticles, which are dispersed in base fluids such as water, ethylene glycol and oil to form nanofluids in order to enhance the heat transfer. Researchers have also used hybrid nanofluids to enhance heat transfer rate along with various inserts such as twisted tape, spiraled rod, wirecoil and many other types and found a drastic increase in the heat transfer rate.

Hwang et al. [2] used Al_2O_3 nanofluid in a plain tube under fully developed laminar flow regime to study the heat transfer enhancement. According to their finding an 8% increase in heat transfer coefficient was obtained at a concentration of 0.3 vol.% compared to pure water. Heris et al. [3] investigated the convective heat transfer of Al_2O_3/water nanofluid in a circular tube and found that the heat transfer coefficient increased with increase in concentration of nanoparticles. Saeedinia et al. [4] studied the thermal and rheological characteristics of CuO − Base oil nanofluids inside a circular tube. The heat transfer coefficient was higher with nanofluids compared with pure oil and a maximum enhancement of 12.7% was obtained with 2 wt.% nanofluids. Hydraulic and heat transfer studies were carried out in horizontal tubes using SiO_2/water nanofluid by Ferrouillat et al. [5]. Their results showed a 10–60% increase in heat transfer coefficient compared to pure water. Duangthongsuk and Wongwises [6] calculated the augmentation of heat transfer and pressure drop characteristics of TiO_2/water nanofluids in a double pipe counter flow heat exchanger and the results showed an enhancement of 6–11% in heat transfer coefficient compared with base fluid. It was also noted that the heat transfer coefficient was directly proportional to the mass flow rate of hot water and nanofluids but inversely proportional to nanofluid temperature. Sonage and Mohanan [7] conducted experiment to find the heat transfer and pressure drop characteristics of Zinc - water nanofluids. Their results showed an increase of 83% in Nusselt number and 9% in pressure drop for the nanofluid compared to water.

Wei Yu et al. [8] investigated the heat transfer performance of Al_2O_3 nanofluids using the mixture of ethylene glycol and water as base fluid and found a 57% and 106% increase in heat transfer coefficient for 1.0 and 2.0 vol.% respectively. Heat transfer and friction factor studies were carried out by Chandrasekar et al. [9] using Al_2O_3/water nanofluids in circular pipe with wire coil inserts. They found an enhancement of 12.24% in Nusselt number with 0.1% volume concentration of nanoparticles at a Reynolds number 2275 compared with water in plain tube. Use of stainless steel wire coil inserts having pitch ratios 2 and 3 with nanofluid led to an enhancement of 15.91 and 21.53% in Nusselt number respectively compared with water in plain tube. Chavan and Pise [10] conducted experimental study to investigate the convective heat transfer enhancement using Al_2O_3/water nanofluids in circular pipe. The heat transfer was found to increase with Reynolds number and nanoparticle concentration. A maximum enhancement of 36% in the heat transfer coefficient was obtained for 1.0 vol.% of nanofluid. Heat transfer behavior of nanofluids in a uniformly heated circular tube fitted with helical twist inserts in laminar flow was numerically studied by Pathipakka and Sivashanmugam [11]. They used helical twist inserts with twist ratios 2.93, 3.91 and 4.89 with 0.5, 1.0 and 1.5 vol.% concentrations of Al_2O_3/water nanofluids for the simulation. It was found that the heat transfer amelioration was directly proportional to Reynolds number and nanoparticles volume concentration and inversely proportional to twist ratio. Maximum heat transfer rate of 31.29% was found for 1.5% volume concentration of nanoparticles with helical tape insert having twist ratio 2.93 at a Reynolds number of 2039. Heat transfer and friction factor were also investigated by Sundar et al. [12] using Fe_3O_4 nanofluid in a plain tube with twisted tape inserts. They found that for 0.6% volume concentration and twist ratio 5, the heat transfer rate was 51.88% higher compared with water for the same Reynolds number. Heyhat et al. [13] conducted heat transfer and pressure drop studies using Al_2O_3/water nanofluids in a horizontal tube. The volume concentration used was 0.1to 2% and laminar flow conditions were maintained. At 2 vol.% of nanofluid, the heat transfer coefficient enhancement was 32% and the pressure drop was higher by 5.7 times compared with DI water.

Saeedinia et al. [14] experimented on the heat transfer and pressure drop of CuO / Base oil nanofluids in a smooth tube with different wire coil inserts under constant heat flux and obtained higher heat transfer rates with nanofluids using wire coil inserts compared with plain tube. With highest wire diameter and 0.3 vol.% of nanofluid, maximum enhancement in heat transfer rate was about 40.2% and the friction factor increase was about 68% in comparison with pure oil in plain tube. Wen and Ding [15] used Al_2O_3/DI water nanofluids in their experimental study on the entrance region under laminar flow conditions. Their results showed considerable enhancement of convective heat transfer using nanofluids. The heat

transfer enhancement was higher in the entrance region and gradually decreased in the axial direction. Suresh et al. [16] investigated the heat transfer enhancement using 0.1 vol.% of Al_2O_3-Cu/DI water hybrid nanofluids. The average enhancement in Nusselt number was 10.94% with hybrid nanofluids compared with DI water. The friction factor also increased by 16.97%.

Teng et al. [17] studied the pressure drop in circular pipes using TiO_2 /water nanofluids for both laminar and turbulent flows at different temperatures and weight fractions of TiO_2.Their results showed the maximum increase in pressure drop for nanofluids was lower under turbulent flow conditions but higher under laminar flow conditions. Rayatzadeh et al. [18] experimented on the influence of continuous sonication on laminar connective heat transfer inside a tube using TiO_2/water nanofluids with 0.10, 0.15 and 0.25% volume concentrations and found that the increase in nanoparticles concentration enhances the heat transfer rate except for 0.25% volume concentration. The Nusselt numbers with 0.25 vol.% of nanofluid and with base fluid are almost similar for the given conditions. Rea et al. [19] investigated the heat transfer and pressure drop of Alumina/water and Zirconia/water nanofluids. The results showed a 17% and 27% enhancement in heat transfer coefficient for entrance and fully developed regions respectively with 6 vol.% of Alumina /water nanofluid whereas the enhancement was 2 and 3% respectively for 1.32 vol.% of Zirconia /water nanofluids. Darzi et al. [20] investigated the turbulent flow characteristics and heat transfer of SiO_2/water nanofluids inside helically corrugated tubes. Their investigation showed maximum heat transfer enhancement when the corrugation height is more and pitch is less. Darzi et al. [21] also conducted a numerical study onAl_2O_3/water nanofluid inside helically corrugated tubes for the turbulent flow regime. Addition of 2% and 4% vol.concentrations nanopartciles in water enhanced the heat transfer by 21% and 58% respectively. Also they obtained an enhancement of 330% in heat transfer using nanofluids with corrugated tubes instead of pure water in plain tube.

In the present work, heat transfer and friction factor characteristics of TiO_2/DI water nanofluids in corrugated tubes under laminar flow conditions are investigated with and without spiraled rod inserts.

2 Experimental methods

2.1 Preparation of TiO_2/DI water nanofluids

TiO_2/DI water nanofluids of various volume concentrations (0.1, 0.15, 0.2 and 0.25%) are prepared by dispersing the TiO_2 nanoparticles in DI water. In order to ensure uniform dispersion and stable suspension of nanoparticles, an ultrasonicator (Toshiba, India) is switched on for a period of 6 h. The sonicator generates ultrasonic frequency of 36 ± 3 KHz. No surfactant is used in the preparation of nanofluids and it is observed that the settlement of nanoparticles even after 15 days is insignificant. This confirms the stability of nanoparticles in DI water.

2.2 Experimental setup

The schematic diagram of experimental facility for the heat transfer and friction factor study is depicted in Fig. 1. The experimental setup includes calming section, test section, riser section, cooling unit, fluid reservoir, pump, temperature, and pressure drop measurement arrangements. The fluid flows from the reservoir by a centrifugal pump. A bypass valve is used to control the rate of flow. The flow rate is measured by using a rotameter. To eliminate entrance effects, the fluid first enters the calming section made of copper tube. The fluid then flows through the test section, riser, cooling section (heat exchanger, cooled by air) and finally collected in the reservoir. A straight copper plain tube and helically corrugated tubes of 1000 mm length, 14 mm inner diameter and 16 mm outer diameter are used as the test section. The geometric specifications of tubes are listed in Table 1. The schematic diagram and photographic view of corrugated tube are shown in Fig. 2(a) and (b).

The test section is heated uniformly with the help of SWG Nichrome electrical heating wire of resistance 120 Ω which is connected to an autotransformer, which controls the heat flux by varying the voltage. Six calibrated temperature sensors (RTD PT 100 type) of 0.1 °C accuracy are placed in the thermowells mounted on the test section to measure the outside wall temperatures. The entry and exit temperatures of the fluid are measured by using calibrated temperature sensors (RTD PT 100 type) immersed in the mixing chambers provided at the inlet and exit. A differential pressure transducer mounted across the test section is used to measure the pressure drop. A differential U-Tube manometer is also fitted across the test section to validate the pressure drop shown by the pressure transducer.

Figure 3 shows the spiraled rod inserts fabricated using 3.5 mm diameter copper rod to which pin like projections of length 10 mm and diameter 2.5 mm are attached at an angle of 22° to the copper rod with pitch of 50 mm (SRI 1) and 30 mm (SRI 2) respectively. An angle of 90° is maintained between two adjacent pins throughout the length of the rod.

2.3 Uncertainty analysis

The experimental Nusselt number and friction factor are subjected to uncertainties due to possible errors in the measured quantities. Uncertainties in the experimental measurement are carried out as per the procedure given by Holman [22]. For

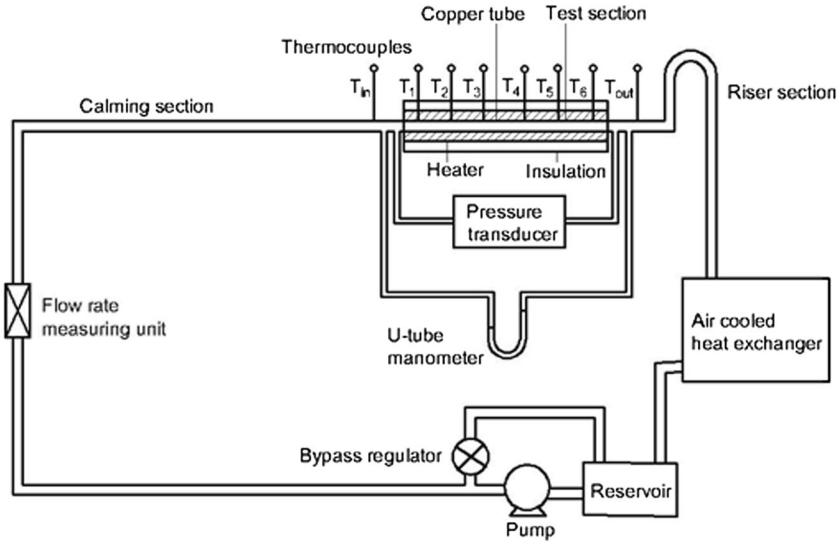

Fig. 1 Schematic diagram of the experimental setup

this purpose, quantities like length of the test section (L), tube diameter (D), pressure drop (ΔP), voltage (V), current (I), mass flow rate (m), wall temperature (T_w) and mean fluid temperature (T_f) are measured and probable errors in each of them are calculated to determine the uncertainties in the experimental data of Nusselt number and friction factor. The calculations show that the uncertainties in the estimation of Reynolds number, Nusselt number and friction factor are ±2.0%, ± 2.83% and ±2.39% respectively.

3 Data reduction

3.1 Thermophysical properties of nanofluids

The commonly used correlations in the literature for the calculation of thermophysical properties of nanofluids are as follows,

The density of TiO_2/DI water nanofluids is found by Pak and Cho's equation [23]

$$\rho_{nf} = \phi\,\rho_s + (1-\phi)\rho \tag{1}$$

Table 1 Geometric specification of tubes (Inside diameter for both plain and corrugated tubes = 14 mm)

HCT No	Corrugation pitch, p_c(mm)	Corrugation height, h_c(mm)
1	8	0.5
2	8	0.75
3	8	1
4	10	1
5	12	1

The specific heat of the nanofluids is found using Xuan and Roetzel's equation [24]

$$\left(\rho\,C_p\right)_{nf} = (1-\phi)\left(\rho\,C_p\right) + \phi\left(\rho\,C_p\right)_s \tag{2}$$

Brookfield viscometer (LVDV-I PRIME C/P) from Brookfield engineering laboratories, USA is used to find the viscosity of nanofluids. The viscosity can also be calculated using Einstein's correlation [25]

$$\mu_{nf} = \mu\,(\,1 + 2.5\,\phi) \tag{3}$$

KD2 Pro thermal property analyser (Decagon Devices, Inc., USA) is used to measure the thermal conductivities of nanofluids. The effective thermal conductivity of the nanofluids, k_{nf} is found using Maxwell equation [26]

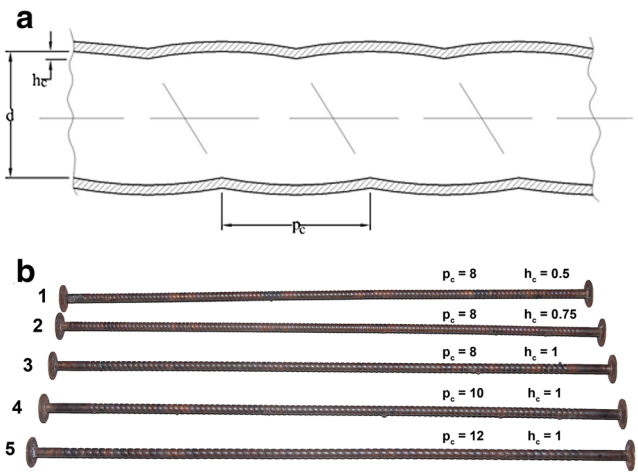

Fig. 2 **a** Schematic diagram of corrugated tube. **b** Photographic view of corrugated tubes

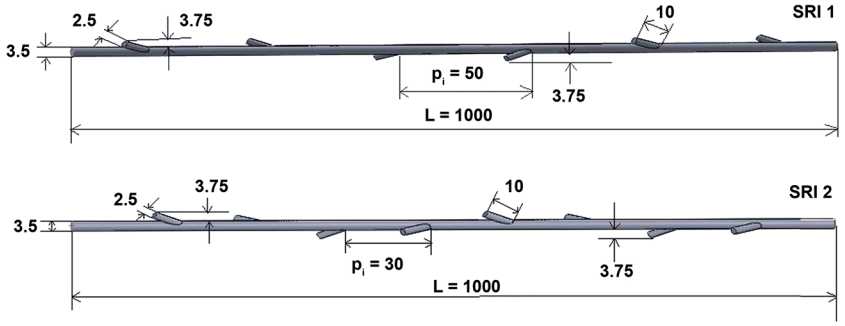

Fig. 3 Geometrical configuration of spiraled rod inserts

$$\frac{k_{nf}}{k} = \frac{k_s + 2k + 2\phi(k_s - k)}{k_s + 2k - \phi(k_s - k)} \tag{4}$$

Thermophysical properties of nanofluids are listed in Table 2.

3.2 Heat transfer calculations

In the laminar flow regime, Nusselt number, friction factor and thermal performance factor are estimated from the experimental data.

The following equation is used to calculate the total heat generated by the electrical winding,

$$Q_t = VI \tag{5}$$

The loss of heat through the insulation (Q_{loss}) is found to be 3.2% of the total heat supplied from the measurements of wall temperature and ambient temperature.

Thus, the actual heat supplied by the heater is,

$$Q_1 = Q_t - Q_{loss} \tag{6}$$

The heat absorbed by the fluid is calculated by the following equation,

$$Q_2 = m\, C_p \left(T_{f,out} - T_{f,in}\right) \tag{7}$$

Heat balance of the actual heat input (Q_1) and the heat carried by the fluid, (Q_2) is within 3.6% for all runs.

The average value of heat transfer rate is calculated as,

$$Q = \frac{(Q_1 + Q_2)}{2} \tag{8}$$

Heat flux is calculated as,

$$q'' = \frac{Q}{(\pi d\, L)} \tag{9}$$

From the equation given below, the local heat transfer coefficient is calculated using local wall temperature, local fluid temperature and heat flux.

$$h_X = \frac{q''}{(T_{wX} - T_{fX})} \tag{10}$$

The fluid temperature at any point is calculated from the energy balance equation given below,

$$T_{fX} = T_{in} + \frac{q'' PX}{\rho C_p v A} \tag{11}$$

The local Nusselt number Nu_x is calculated as,

$$Nu_X = \frac{h_X\, d}{k} \tag{12}$$

The average heat transfer coefficient is calculated using average wall temperature, mean fluid temperature and heat flux from the equation given below,

$$h = \frac{q''}{\left(T_w - T_f\right)} \tag{13}$$

Here, T_w is the average temperature of the wall and T_f is the mean temperature of fluid.

Table 2 Thermophysical properties of TiO_2/DI water nanofluids at room temperature

Properties	0.1 vol.%	0.15 vol.%	0.2 vol.%	0.25 vol.%
Density (kg/m^3)	1003.25	1004.88	1006.5	1008.13
Thermal conductivity (W/m K)	0.617	0.620	0.628	0.640
Dynamic viscosity (mPa s)	0.92	0.96	1.02	1.07
Specific heat (J/kg K)	4163.22	4155.85	4148.54	4141.22

The average Nusselt number is calculated as below,

$$Nu = \frac{h\,d}{k} \tag{14}$$

Thermal resistance is calculated as,

$$R = \frac{\left(T_w - T_f\right)}{q''} \tag{15}$$

3.3 Pressure drop calculations

The pressure drop (Δp) is measured using a U-tube manometer. Friction factor is calculated under isothermal conditions using the equation given below,

$$f = \frac{\Delta p}{\left(\frac{1}{2}\,\rho\, v^2\right)}\left(\frac{d}{L}\right) \tag{16}$$

4 Results and discussion

4.1 Validation of experimental setup

Experiments are carried out under laminar flow conditions in plain tube using DI water to validate the experimental setup. The results are compared with Shah Equation for constant heat flux boundary conditions and there is a good agreement between them. The variation of experimental and theoretical Nusselt number along the axial direction at a Reynolds number of 610 is shown in Fig. 4. Shah equation is given [27] as,

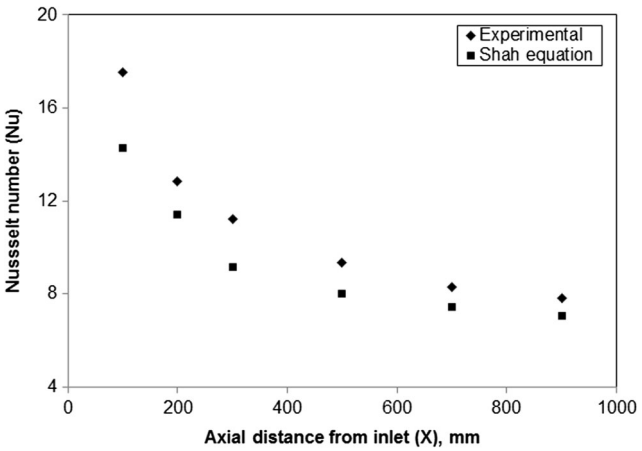

Fig. 4 Variation of Nusselt number along the axial direction at a Reynolds number of 610

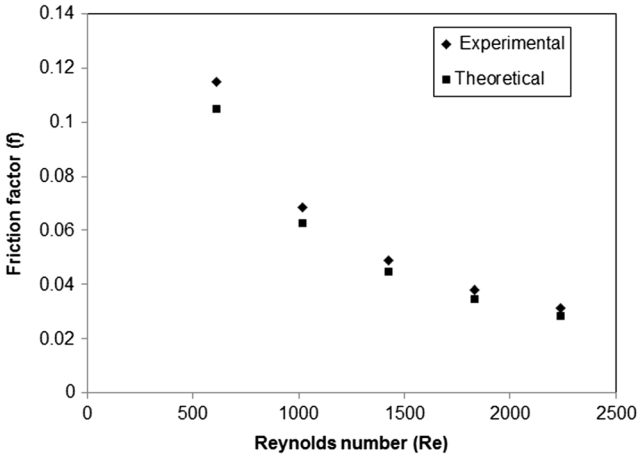

Fig. 5 Comparison of experimental friction factor with the theoretical values

$$Nu = 1.953\left(\mathrm{Re\,Pr}\,\frac{d}{X}\right)^{1/3} \; for\left(\mathrm{Re\,Pr}\,\frac{d}{X}\right) \geq 33.33 \tag{17}$$

$$Nu = 4.364 + 0.0722\left(\mathrm{Re\,Pr}\,\frac{d}{X}\right) \quad for\left(\mathrm{Re\,Pr}\,\frac{d}{X}\right) \leq 33.33 \tag{18}$$

Hagen-Poiseuille equation is used to compare the experimental and theoretical friction factors as shown in the Fig. 5.

The friction factor is given by,

$$f = \frac{64}{\mathrm{Re}} \tag{19}$$

4.2 Heat transfer studies

Figure 6 depicts the Nusselt number variation with Reynolds number for plain tube with and without spiraled rod inserts. It

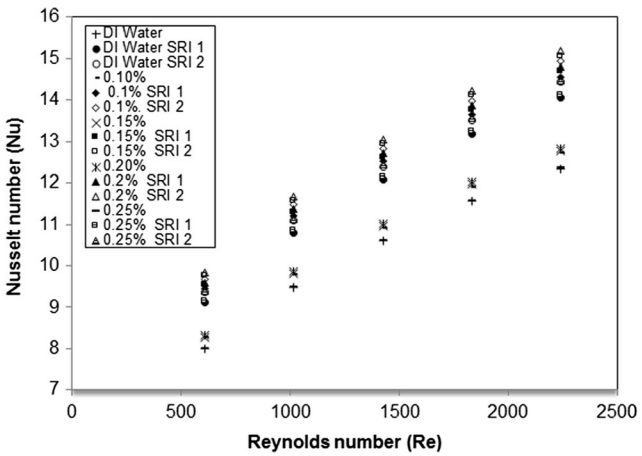

Fig. 6 Variation of Nusselt Number with Reynolds number for plain tube

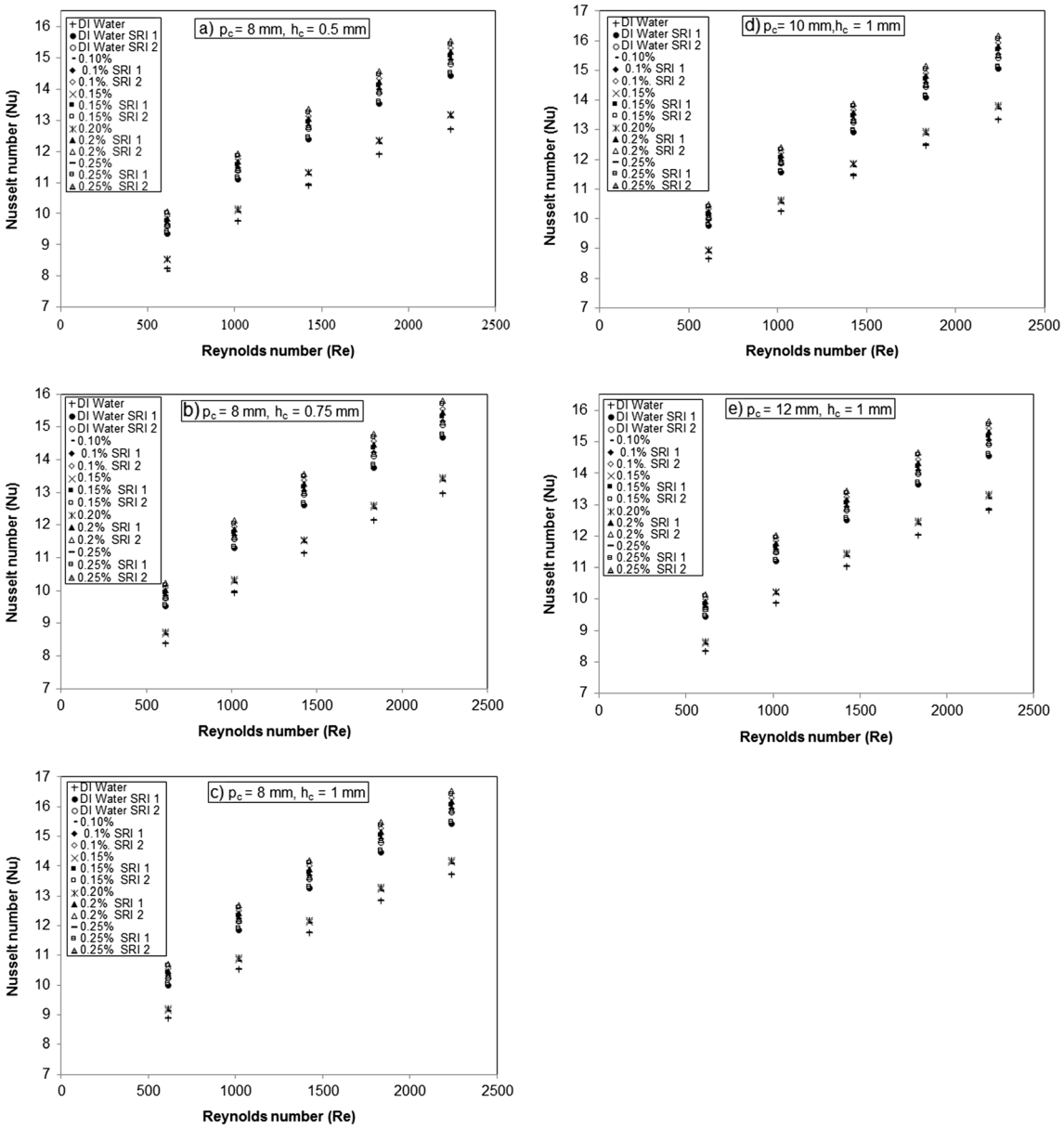

Fig. 7 Variation of Nusselt number with Reynolds number for corrugated tubes. **a** Tube 1 **b** Tube 2 **c** Tube 3 **d** Tube 4 **e** Tube 5

can be clearly seen that the Nusselt number increases with Reynolds number in the case of DI water. TiO_2/DI water nanofluids of 0.1, 0.15, 0.2, and 0.25% volume concentrations are studied in this work. Addition of nanoparticles has a positive impact on Nusselt number except for 0.25% volume concentration. The enhancement in Nusselt number for 0.1, 0.15 and 0.2% volume concentrations of nanofluids are 3.03, 3.6 and 4% respectively compared to DI water. But for 0.25% volume concentration of nanofluid, it is approximately same as that of DI water.

The enhancement in Nusselt number due to the addition of nanoparticles are mainly attributed to the decrease of boundary layer thickness and delayed growth of boundary layer, increased thermal conductivity, Brownian motion, migration

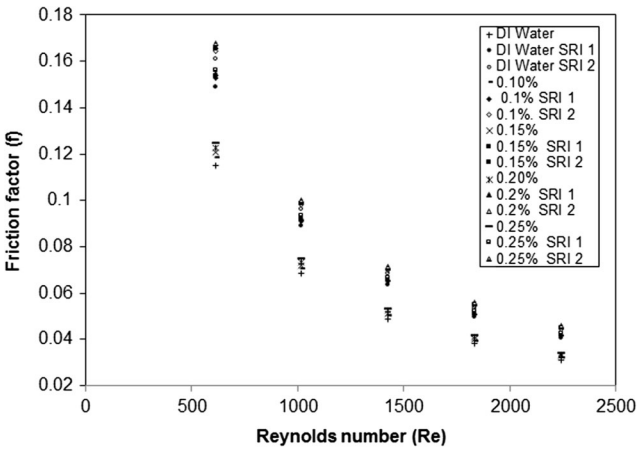

Fig. 8 Variation of friction factor with Reynolds number for plain tube

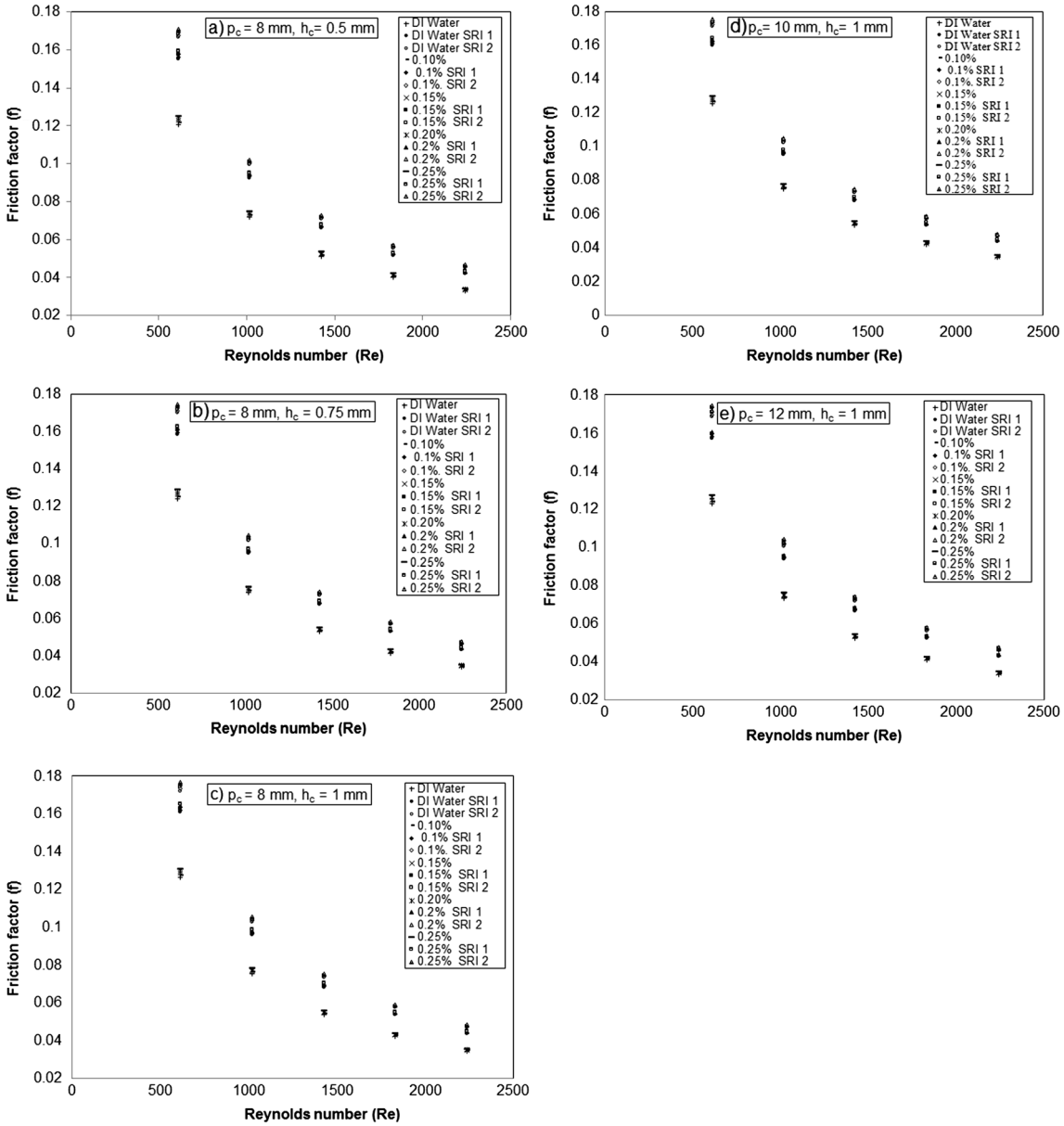

Fig. 9 Variation of friction factor with Reynolds number for corrugated tubes. **a** Tube 1 **b** Tube 2 **c** Tube 3 **d** Tube 4 **e** Tube 5

and rearrangement of particles and large energy exchange due to chaotic motion of particles [9]. In laminar flow regime, higher concentration of nanoparticles increases the viscosity and thus boundary layer thickness leading to a decrease in Nusselt number. Hence, 0.25% volume concentration of nanofluids has no significant enhancement in Nussselt number, which is similar to the findings of Rayatzadeh et al. [18].

Addition of spiraled rod inserts in plain tube further enhances the Nusselt number compared with DI water in plain tube. Two inserts having pitches of 50 mm (SRI 1) and 30 mm (SRI 2) are used in this study for the heat transfer enhancement. The Nusselt number is found to increase in both cases compared to DI water in plain tube. The Nusselt number also increases with decrease in pitch of inserts. The enhancement in Nusselt number is 14 and 17% for SRI 1 and SRI 2 respectively. It can be perceived from the Fig. 6 that the use of spiraled rod inserts with nanofluids enhances the Nusselt number further compared to plain tube. The enhancement in Nusselt number obtained is 18.02, 19 and 20% for 0.1, 0.15 and 0.2% volume concentrations with SRI 1 and 21, 22.02, 23% for SRI 2 compared to DI water in plain tube.

The heat transfer augmentation due to the inserts is mainly because of the following reasons:

(1) The pins attached on the rod act as turbulent promoters
(2) Development of secondary flows
(3) Reduction in hydraulic diameter

(4) Enhanced energy exchange in the fluids due to irregular and random movement of the particles.
(5) Excellent fluid mixing and an efficient redevelopment of the thermal and hydrodynamic boundary layers due higher turbulence intensity close to the tube wall.

Heat transfer rate is augmented further with the use of helically corrugated tubes. Fig. 7(a − e) shows the variation of Nusselt number with Reynolds number for corrugated tubes with and without inserts. The enhancement in Nusselt number obtained for HCT 1 is 3.06, 6, 6.7 and 7.02% for DI water, 0.1, 0.15 and 0.2% volume concentration of nanofluids respectively compared to DI water in pain tube. The volume concentration of 0.25% also enhances the Nusselt number compared to plain tube with same concentration. Similarly for HCT 2, the enhancement is 5.01, 8.06, 8.6 and 9.02% for DI water, 0.1, 0.15 and 0.2% respectively compared to DI water in plain tube. The maximum enhancement is obtained for HCT3, which has the maximum corrugation height and minimum pitch and the corresponding Nusselt number values are 11, 14, 14.5 and 15%. Increasing the corrugation pitch reduces the the Nusselt number. Accordingly, the values of Nusselt number enhancement are 8.01, 11, 11.6, 12% and 4.01, 7.01, 7.6 and 8.02% for HCT4 and HCT 5 respectively.

Nusselt number of HCTs fitted with spiral rod inserts is considerably improved when compared with that of the HCT without inserts. The enhancement in Nusselt number for HCT 1 with SRI 1 and SRI 2 for 0.2% volume concentration is 23.08 and 26.01% respectively. Similarly for HCT 2, the enhancement is 25.08 and 28.01%. The corresponding enhancement for HCT 3–5 are 31.08 and 34%; 28.08 and 31.01%; 24.08 and 27.01% respectively.

Among the corrugated tubes, maximum Nusselt number enhancement is obtained with the tube of lowest pitch and maximum height of corrugation ($p_c = 8$ mm, $h_c = 1$ mm). A maximum increase of 34% in Nusselt number is found for the above tube with 0.2% volume concentration of nanofluids and SRI 2 ($p_i = 30$ mm). This enhancement is credited to the combined effects of corrugation on the tube wall, nanofluid and inserts. The use of SRI and HCT provide large area of contact with fluid and wall. Also it helps in better dispersion of nanoparticles and its random movement leading to good mingling between the core fluid and the one near the tube wall, which is the reason for heat transfer enhancement.

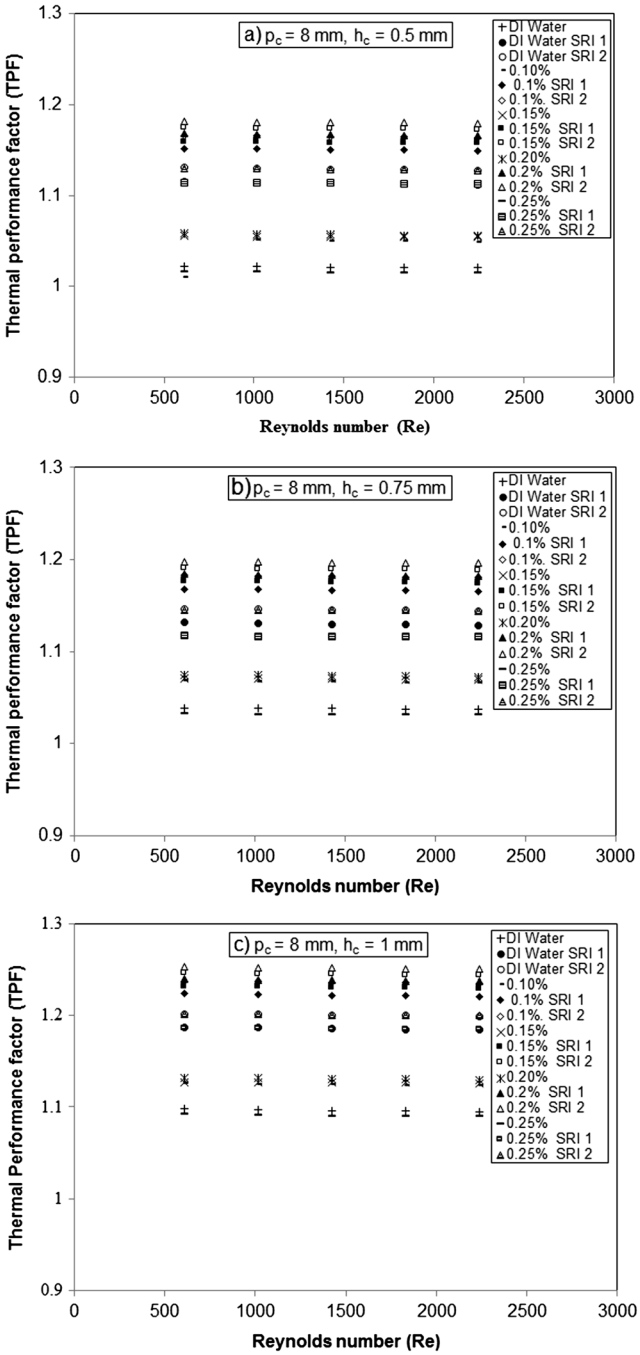

Fig. 10 Variation of thermal performance factor with Reynolds number for corrugated tubes. **a** Tube 1 **b** Tube 2 **c** Tube 3 **d** Tube 4 **e** Tube 5

4.3 Pressure drop studies

The use of nanofluids though increases the heat transfer performance, it is also essential to measure the pressure drop in order to use them in industrial applications. Hence, the pressure drops of nanofluid in a plain tube and HCTs at different flow rates are experimentally measured and the friction factor is calculated. Friction factor variations with the Reynolds number are shown in Fig. 8 for plain tube. Friction factor decreases with increasing Reynolds number in all the cases. Friction factor slightly increases with the addition of nanoparticles due to the increased shear force between the wall and the nanoparticles and also due to increased viscosity. But the increase in friction factor is not significant compared

with DI water and hence the pressure drop penalty is negligible. Friction factor increases with the volume concentrations of nanofluids and the increase for 0.1, 0.15, 0.2 and 0.25% volume concentrations are 3.2, 5.09, 7.8 and 8.8% respectively compared with DI water.

Friction factor further increases in plain tube fitted with spiraled rod inserts. The rise in friction factor in the case of plain tubes with DI water, 0.1, 0.15, 0.2 and 0.25% volume concentrations of nanofluids are 30.65, 33.08, 34.7, 35.7 and 36.7% for SRI 1 and 40.8, 43.09, 44.7, 45.7 and 46.8% for SRI 2 compared to DI water without inserts. Use of inserts increases the friction factor for both DI water and nanofluid. The pitch of spiraled rod inserts plays a significant role in the friction factor, increasing pitch reduces the friction factor. This is due to the geometry and larger contact surface. Also, the inserts reduce the free flow area and induces turbulence in the flow. This leads to increased friction between the surface of the core rod and the inner wall of the tube.

Figure 9(a − e) shows the effect of Reynolds number, inserts and nanoparticles on friction factor for corrugated tubes. The corrugation in the tube wall increases the friction factor. Among the corrugated tubes, the HCT with lower pitch and higher height of corrugation (HCT 3, $p_c = 8$ mm, $h_c = 1$ mm) has the highest friction factor. The friction factor for the HCT 3 with DI water is 10.7% more compared with DI water in plain tube and it further increases with inserts and nanoparticles. The maximum increase in friction factor for DI water, 0.1, 0.15, 0.2 and 0.25% volume concentrations of nanofluids are 40.66, 41.58, 42.57, 43.54 and 44.57% with SRI 1 and 50.57, 51.7, 52.67, 53.56 and 54.67% with SRI 2 respectively compared with DI water in plain tube.

4.4 Thermal performance analysis

Figure 10(a − e) shows the thermal performance analysis of spiraled rod inserts under laminar flow conditions for TiO_2/DI water nanofluids in HCT. The Thermal Performance Factor (TPF) for same pumping power in laminar flow is given by the correlation of Usui et al. [28]

$$\eta = \frac{\left(\frac{Nu_{HCT}}{Nu_{pt}}\right)}{\left(\frac{f_{HCT}}{f_{pt}}\right)^{0.1666}} \tag{20}$$

The thermal performance factor increases with the use of inserts due to the generation of turbulence, which becomes stronger when the pitch is reduced. In the case of HCT, the TPF increases with increasing corrugation height and decreasing corrugation pitch.

The TPF decreases with increasing Reynolds number because of increased pressure loss at higher Reynolds number increases. For the range of Reynolds number studied, the TPF is greater than unity for all the HCTs with and without inserts. A maximum thermal performance of 1.25 is found for HCT3 having $p_c = 8$ mm and hc = 1 mm with 0.2% volume concentration of nanofluid inserted with spiraled rod having lower pitch ($p_i = 30$ mm).

5 Conclusions

The experimental investigation on heat transfer augmentation using TiO_2/DI water nanofluids in helically corrugated tubes with and without spiraled rod inserts under laminar flow leads to the following conclusions:

1. The heat transfer rate, friction factor and thermal performance factor associated with combined applications of TiO_2/DI water nanofluids with spiraled rod inserts and HCT are higher than the individual techniques.
2. Heat transfer rate, friction factor and thermal performance factor increase with an increase in TiO_2 particles concentration upto 0.2%. Increase in corrugation height and decrease in pitch of both HCT and inserts also increase the above factors.
3. For 0.2% volume concentration, the maximum increase in heat transfer rate in plain tube with and without inserts are 23% and 4% respectively whereas the maximum heat transfer augmentation of 34% and 15% is found for the HCT 3 with and without inserts.
4. Pressure drop of nanofluids compared with water is almost negligible which shows that the nanofluids incur no pumping power penalty.

References

1. Choi SUS (1995) Enhancing thermal conductivity of fluid with nanoparticles. In: Signer DA, Wang HP (eds) Developments and Applications of Non-Newtonian Flows, FED-vol.231/MD-vol.66. ASME, New York, pp 99–105
2. Hwang KS, Jang SP, Choi SUS (2009) Flow and convective heat transfer characteristics of water-based Al_2O_3nanofluids in fully developed laminar flow regime. Int J Heat Mass Transf 52:193–199
3. Zeinali Heris S, Nasr Esfahany M, Etemad SG (2007) Experimental investigation of convective heat transfer of Al_2O_3/water nanofluid in circular tube. Int J Heat Fluid Flow 28:203–210
4. Saeedinia M, Akhavan-Behabadi MA, Razi P (2012) Thermal and rheological characteristics of CuO-Base oil nanofluid flow inside a circular tube. Int Commun Heat Mass Transf 39:152–159
5. Ferrouillat S, Bontemps A, Ribeiro J-P, Gruss J-A, Soriano O (2011) Hydraulic and heat transfer study of SiO_2/ water nanofluid in horizontal tubes with imposed wall temperature boundary conditions. Int J Heat Fluid Flow 32:424–439
6. Duangthongsuk W, Wongwises S (2009) Heat transfer enhancement and pressure drop characteristics of TiO_2− water nanofluid

in a double-tube counter flow heat exchanger. Int J Heat Mass Transf 52:2059–2067
7. Sonage BK, Mohanan P (2015) Heat transfer and pressure drop characteristics of zinc-water nanofluid. Heat Mass Transf 51(4): 521–527
8. Yu W, Xie H, Yang L, Chen L, Wang Q (2012) Experimental investigation on the heat transfer properties of Al_2O_3 nanofluids using the mixture of ethylene glycol and water as base fluid. Powder Technol 230:14–19
9. Chandrasekar M, Suresh S, Chandra Bose A (2012) Experimental studies on heat transfer and friction factor characteristics of Al_2O_3/water nanofluid in a circular pipe under laminar flow with wire coil insert. Exp Thermal Fluid Sci 34:122–130
10. Chavan D, Pise AT (2015) Experimental investigation of convective heat transfer augmentation using Al_2O_3/water nanofluid in circular pipe. Heat Mass Transf 51(9):1237–1246
11. Pathipakka G, Sivashanmugam P (2012) Heat transfer behavior of nanofluids in a uniformly heated circular tube fitted with helical inserts in laminar flow. Superlatti Microstruct 47:349–360
12. Syam Sundar L, Ravi Kumar NT, Naik MT, Sharma KV (2012) Effect of full length twisted tape inserts on heat transfer and friction factor enhancement with Fe_3O_4 magnetic nanofluid inside a plain tube: An experimental study. Int J Heat Mass Transf 55:2761–2768
13. Heyhat MM, Kowsary F, Rashidi AM, Momenpour MH, Amrollahi A (2013) Experimental investigation of laminar convective heat transfer and pressure drop of water-based Al_2O_3 nanofluids in fully developed flow regime. Exp Thermal Fluid Sci 44:483–489
14. Saeedinia M, Akhavan-Behabadi MA, Nasr M (2012) Experimental study on heat transfer and pressure drop of nanofluid flow in a horizontal coiled wire inserted tube under constant heat flux. Exp Thermal Fluid Sci 36:158–168
15. Wen D, Ding Y (2004) Experimental investigation into convective heat transfer of nanofluids at the entrance region under laminar flow conditions. Int J Heat Mass Transf 47:5181–5188
16. Suresh S, Venkitaraj KP, Selvakumar P, Chandrasekar M (2012) Effects of Al_2O_3−Cu/water hybrid nanofluid in heat transfer. Exp Thermal Fluid Sci 38:54–60
17. Teng T-P, Hung Y-H, Jwo C-S, Chen C-C, Jeng L-Y (2011) Pressure drop of TiO_2 nanofluid in circular pipes. Particu 9:486–491
18. Rayatzadeh HR, MajidSaffar-Avval MM, Abbassi A (2013) Effects of continuous sonication on laminar convective heat transfer inside a tube using water- TiO_2 nanofluid. Exp Thermal Fluid Sci 48:8–14
19. Rea U, McKrell T, Hu L-w, Buongiorno J (2009) Laminar convective heat transfer and viscous pressure loss of alumina-water and zirconia-water nanofluids. Int J Heat Mass Transf 52:2042–2048
20. Rabienataj Darzi AA, Farhadi M, Sedighi K, Shafaghat R, Zabihi K (2012) Experimental investigation of turbulent heat transfer and flow characteristics of SiO_2/water nanofluid within helically corrugated tubes. Int Commu Heat Mass Transf 39:1425–1434
21. Rabienataj Darzi AA, Farhadi M, Sedighi K, Aallahyari S, Delavar MA (2013) Turbulent heat transfer of Al_2O_3-water nanofluid inside helically corrugated tubes: Numerical study. Int Commu Heat Mass Transf 41:68–75
22. Holman JP (2001) Experimental Methods for Engineers, 7th edn. McGraw-Hill, New York (Chapter 3)
23. Pak BC, Cho Y (1998) Hydrodynamic and heat transfer study of dispersed fluids with submicron metallic oxide particle. Exp Heat Transf 11:151–170
24. Xuan Y, Roetzel W (2000) Conceptions of heat transfer correlation of nanofluids. Int J Heat Mass Transf 43:3701–3707
25. Einstein A (1956) Investigation on the theory of Brownian motion. Dover, New York
26. Maxwell JC (1954) Treaties on Electricity and Magnetism. Dover, New York
27. Shah RK (1975) Thermal entry length solutions for the circular tube and parallel plates. In: Proceedings of Third National Heat And Mass Transfer Conference, Indian Institute of Technology, Bombay, p. 1 (Paper No. HMT−11−75)
28. Usui H, Sano Y, Iwashita K, Isozaki A (1996) Enhancement of heat transfer by a combination of internally grooved rough tube and twisted tape. Int Chem Eng 26(1):97–104